the exo-anilino case. Thus, there is no doubt that the yellow product is indeed exo.

The endo-phosphonium isomer, studied in deuteriodichloromethane, shows the narrowing of the H_5 signal, behavior analogous to that in the endo-anilino case. On irradiation of H_5, H_4 collapses and the low-field diene region H_3 is affected. It is clear that the coupling between H_4 and H_5 is not longer zero. Thus the brown product is 5-endo.

The NMR spectra of the other phosphonium complexes can be assigned in a similar manner.

The ^{13}C results (Table III) substantiated the above. Except for very small differences in the chemical shifts, both isomers display similar patterns. However, a variation in the coupling constants of ^{31}P with the neighboring carbon atoms C_4 and C_5 is observed in the ethylphosphine case. Although it is not possible to correlate this result with a particular geometrical configuration, it does indicate the expected change in orientation of the phosphorus group between the isomers.

These results show clearly that substitution of the tricarbonyl(η-1,5-cycloheptadienylium)iron cation by phosphines yields both the 5-exo and 5-endo isomers depending on reaction conditions. The presence of a red coloration during reaction in acetonitrile and during the interconversion of exo to endo isomer is consistent with metal-assisted substitution. The inability of phenyl-substituted phosphines to form the 5-endo isomer is presumably due to steric inhibition of the metal-assisted pathway. In contrast, substitution in dichloromethane proceeds by direct ring attack to give the 5-exo isomer.

In conclusion, the general pattern of nucleophilic substitution of both hard and soft nucleophiles is in good accord with the theoretical discussion of the preceding paper. Thus by varying the nucleophilicity of the attacking group it is possible to observe both metal and carbonyl carbon attack and formation of stable products. It is also possible for hard nucleophiles to attack at the carbonyl carbon atom (and possibly at the metal atom also) even if the final thermodynamically stable product is ring substituted. Finally, for soft nucleophiles such as phosphines, both ring isomers may be obtained although even in this case there may be a metal-assisted pathway in the formation of the endo isomer.

Registry No. I, 12212-05-4; II, R = Et, 81522-88-5; II, R = Me, 81522-89-6; II, R = *i*-Pr, 81522-90-9; 5-*exo*-$C_7H_9OEtFe(CO)_3$, 12109-81-8; $C_7H_9Fe(CO)_2NCO$, 81522-91-0; $C_7H_9Fe(CO)_2CONHNH_2$, 81522-92-1; $[C_7H_9Fe(CO)_2NH_2N(CH_2Ph)_2]BF_4$, 81522-94-3; 5-*exo*-*n*-$PrNH_2C_7H_9Fe(CO)_3]BF_4$, 81522-80-7; 5-*exo*-*n*-$PrNHC_7H_9Fe(CO)_3$, 81522-79-4; [5-*exo*-$PEt_3C_7H_9Fe(CO)_3]BF_4$, 81534-79-4; [5-*endo*-$PEt_3C_7H_9Fe(CO)_3]BF_4$, 81600-18-2; 5-*exo*-$MeOC_7H_9Fe(CO)_3$, 81570-96-9; 5-*exo*-*i*-$PrOC_7H_9Fe(CO)_3$, 81522-81-8; $[C_7H_9Fe(CO)_2NH_2N(CH_2$-*p*-$NO_2C_6H_4)_2]BF_4$, 81522-83-0; $[C_7H_9Fe(CO)_2NH_2N(CH_2$-*p*-$MeOC_6H_4)_2]BF_4$, 81534-81-8; [5-*exo*-P(*n*-Pr)$_3C_7H_9Fe(CO)_3]BF_4$, 81522-85-2; [5-*endo*-P(*n*-Pr)$_3C_7H_9Fe(CO)_3]BF_4$, 81570-98-1; [5-*exo*-P(*n*-Bu)$_3C_7H_9Fe(CO)_3]BF_4$, 81570-86-7; [5-*endo*-P(*n*-Bu)$_3C_7H_9Fe(CO)_3]BF_4$, 81570-88-9; [5-*exo*-$PMe_2PhC_7H_9Fe(CO)_3]BF_4$, 81522-76-1; [5-*endo*-$PMe_2PhC_7H_9Fe(CO)_3]BF_4$, 81570-90-3; [5-*exo*-$PEtPh_2C_7H_9Fe(CO)_3]BF_4$, 81522-78-3; [5-*exo*-$PPh_3C_7H_9Fe(CO)_3]BF_4$, 81570-92-5; [5-*exo*-*n*-$BuNH_2C_7H_9Fe(CO)_3]BF_4$, 81570-93-6; [5-*exo*-*t*-$BuNH_2C_7H_9Fe(CO)_3]BF_4$, 81600-03-5; [5-*exo*-$Et_2NHC_7H_6Fe(CO)_3]BF_4$, 81570-94-7; [5-*exo*-$C_4H_8NHC_7H_9Fe(CO)_3]BF_4$, 81570-95-8; [5-*exo*-$C_5H_{10}NHC_7H_9Fe(CO)_3]BF_4$, 81522-70-5; [5-*exo*-$C_5H_5NC_7H_9Fe(CO)_3]BF_4$, 81570-83-4; 5-*exo*-*n*-$BuNHC_7H_9Fe(CO)_3$, 81522-71-6; 5-*exo*-*t*-$BuNHC_7H_9Fe(CO)_3$, 81570-84-5; 5-*exo*-$Et_2NC_7H_9Fe(CO)_3$, 81522-72-7; 5-*exo*-$C_4H_8NC_7H_9Fe(CO)_3$, 81522-73-8; 5-*exo*-$PhNHC_7H_9Fe(CO)_3$, 67711-11-9; 5-*exo*-$PhNMeC_7H_9Fe(CO)_3$, 81522-74-9.

Contribution from the Department of Chemical Engineering, Tokyo Institute of Technology, Ookayama, Meguro-ku, Tokyo 152, Japan

Metal Cluster Catalysis. Kinetics and Mechanism of the Catalytic Hydrogenation of Ethylene by the Ruthenium Cluster Complex $H_4Ru_4(CO)_{12}$

YOSHIHARU DOI,* KUNIHIRO KOSHIZUKA, and TOMINAGA KEII

Received March 31, 1981

The tetraruthenium cluster hydride $H_4Ru_4(CO)_{12}$ reacts with ethylene at 72 °C to give two molecules of ethane per molecule of cluster. In the presence of excess hydrogen, this cluster complex acts as a catalyst for the hydrogenation of ethylene in heptane solution. Detailed kinetics for the catalytic hydrogenation are presented as functions of catalyst concentration, ethylene pressure, hydrogen pressure, and carbon monoxide pressure. In the reaction of C_2H_4 with D_2, the hydrogen–deuterium exchange between reactants takes place to give C_2H_3D and HD by a more rapid rate than that of ethane formation. A reasonable catalytic cycle for the ethylene hydrogenation is proposed to involve $H_3Ru_4(CO)_{11}(C_2H_5)$ as an intermediate.

Introduction

Mononuclear transition-metal compounds have been extensively used as homogeneous catalysts for the hydrogenation of olefins. The mechanism of olefin hydrogenation on mononuclear transition-metal complexes is well established and has been reviewed by James.[1] Recently, the use of transition-metal cluster compounds as homogeneous catalysts for the olefin hydrogenation has been increasing. Examples include the hydrogenation of olefins with molecular clusters of ruthenium,[2-6] osmium,[7,8] rhodium,[9] and nickel.[10] These metal clusters are considered to provide polymetallic active sites for the catalytic reactions. Recent publications[11-13] have pointed out the analogies between molecular metal clusters and metal surfaces in the processes of chemisorption and of catalysis. At

(1) James, B. R. "Homogeneous Hydrogenation"; Wiley: New York, 1973.
(2) Valle, M.; Osella, D.; Vaglio, G. A. *Inorg. Chim. Acta* **1976**, *20*, 213.
(3) Lausarot, P. M.; Vaglio, G. A.; Valle, M. *Inorg. Chim. Acta* **1979**, *36*, 213.
(4) Botteghi, C.; Gladiali, S.; Bianch, M. Matteoli, U.; Frediani, P.; Vergamini, P. G.; Benedetti, E. *J. Organomet. Chem.* **1977**, *140*, 221.
(5) Graff, J. L.; Wrighton, M. S. *J. Am. Chem. Soc.* **1980**, *102*, 2123.
(6) Fouda, S. A.; Rempel, G. L. *Inorg. Chem.* **1979**, *18*, 1.
(7) Keister, J. B.; Shapley, J. R. *J. Organomet. Chem.* **1975**, *85*, c29; *J. Am. Chem. Soc.* **1976**, *98*, 1056.
(8) Deeming, A. J.; Hasso, S. *J. Organomet. Chem.* **1976**, *114*, 313.
(9) Reinman, W.; Abboud, W.; Basset, J. M.; Mutin, R.; Rempel, G. L.; Smith, A. K. *J. Mol. Catal.* **1980**, *9*, 349.
(10) Muetterties, E. L.; Band, E.; Kokorin, A.; Pretzer, W. R.; Thomas, M. G. *Inorg. Chem.* **1980**, *19*, 1552.
(11) Ugo, R. *Catal. Rev.* **1975**, *11*, 225.
(12) Muetterties, E. L. *Science (Washington, D.C.)* **1977**, *196*, 839.
(13) Muetterties, E. L.; Rhodin, T. N.; Band, E.; Brucker, C. F.; Pretzer, W. R. *Chem. Rev.* **1979**, *79*, 91.

0020-1669/82/1321-2732$01.25/0

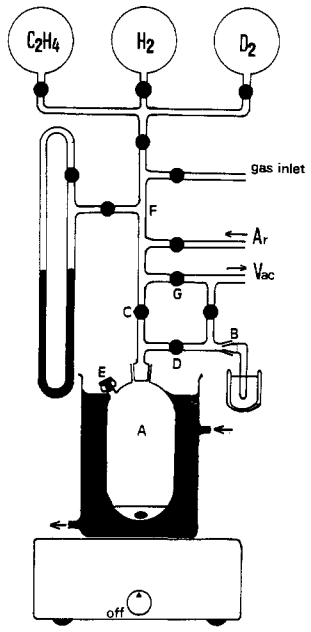

Figure 1. Schematic diagram of the reaction system.

the present time, however, mechanistic investigations concerning the catalysis by metal clusters are very few. One of the most thorough studies of metal cluster catalysis is the work[7] of Keister and Shapley, who established the catalytic cycle for olefin hydrogenation in the presence of $H_2Os_3(CO)_{10}$, which contains an osmium–osmium double bond and allows coordination of the olefin molecule. Aside from $H_2Os_3(CO)_{10}$, many stable metal clusters including $H_4Ru_4(CO)_{12}$ are coordinately and sterically saturated. For these catalyst precursors, first steps to initiate a catalytic cycle comprise the dissociation of a ligand-like carbon monoxide[2,5,14] or the cleavage of one metal–metal bond resulting in an open butterfly structure.[15,16]

In order to further the understanding of metal cluster catalysis, we have made a comparative study on the stoichiometric and catalytic hydrogenation of ethylene with $H_4Ru_4(CO)_{12}$. Detailed kinetics of ethylene hydrogenation are presented along with the mechanistic implications of metal cluster catalysis.

Experimental Section

Materials. The complex $H_4Ru_4(CO)_{12}$ and its deuterated analogue were prepared by a reported method.[17] Ethylene, Takachio ultra pure grade, was dried by passing it through a column of 4A molecular sieve. Hydrogen, deuterium (purity 99.5%), and carbon monoxide were purchased from Takachio Co. and used without further purification. Argon of pure grade was used after passage through a column of copper reduced at 350 °C. Heptane, Wako pure grade, was dried on 4A molecular sieve and saturated with dry argon prior to use.

Apparatus and Procedure. The apparatus used for hydrogenation study is shown schematically in Figure 1. A typical experiment is described below. (i) A prescribed amount of ethylene was introduced into the reaction vessel A (ca. 257 cm^3) with a Teflon-coated stirring bar. After the greaseless stopcock C was closed, ethylene in the vessel A was collected in a trap B (ca. 9 cm^3) by freezing, and then stopcock D was closed. (ii) In all experiments, 5 cm^3 of a heptane solution of $H_4Ru_4(CO)_{12}$ or $D_4Ru_4(CO)_{12}$ in the range of concentrations between 0.1 and 1.2 mM was admitted in the reaction vessel through the side arm E by syringe under an argon stream, and again the side arm E was sealed by silicon rubber packing. (iii) The ruthenium cluster solution in the reaction vessel was cooled to −78 °C, and then argon gas was evacuated via stopcock G. After stopcocks G and C were closed, hydrogen or deuterium gas was introduced in the part F (ca. 140 cm^3) and precisely measured by a mercury-leveling manometer. A known amount of hydrogen or deuterium was admitted into the reaction vessel A via stopcock C. (iv) After stopcock C was closed, the reaction vessel was immersed in an oil bath and allowed to stand for 15 min at a reaction temperature. The temperature of the oil bath was controlled to ±0.3 °C. Then, a known amount of ethylene was added into the reaction vessel by heating trap B, and stopcock D was closed. The hydrogenation reaction was timed from the addition of ethylene. Vigorous agitation of the catalyst solution caused no appreciable change in the hydrogenation rate, even for the highest rate studied. When required, carbon monoxide was introduced through the silicon rubber seal E by a syringe.

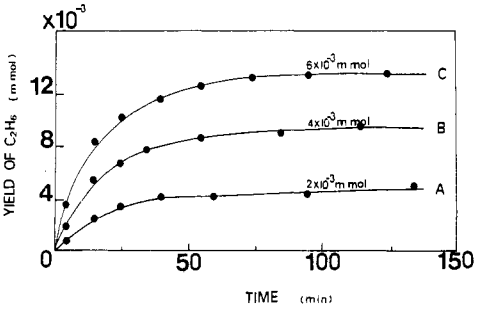

Figure 2. Yield of C_2H_6 produced during the reaction of C_2H_4 with $H_4Ru_4(CO)_{12}$ (72 °C, $P_{C_2H_4}$ = 100 torr, heptane solution = 5 mL): A, $H_4Ru_4(CO)_{12} = 2 \times 10^{-3}$ mmol; B, $H_4Ru_4(CO)_{12} = 4 \times 10^{-3}$ mmol; C, $H_4Ru_4(CO)_{12} = 6 \times 10^{-3}$ mmol.

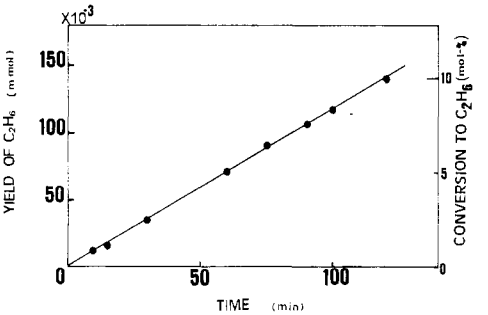

Figure 3. Representative C_2H_6 yield plot for the catalytic hydrogenation of ethylene with $H_4Ru_4(CO)_{12}$. Reaction conditions: 72 °C, $P_{C_2H_4}$ = 100 torr, P_{H_2} = 100 torr, and 0.4 mM solution of $H_4Ru_4(CO)_{12}$ (5 mL).

Product Analysis. Samples of the gases above the reaction solution were withdrawn at intervals by a syringe and analyzed quantitatively on a Hitachi 163 FID gas chromatograph with a 2-m column of Porapak Q. For the reaction of ethylene with deuterium, deuterated products were also separated by gas chromatography and analyzed by a Hitachi RMU-7M mass spectrometer. Infrared spectra of reaction solutions were recorded on a Hitachi 295 spectrometer. Electronic absorption spectra were recorded on a Shimazu MPS-5000 spectrophotometer.

Results

Stoichiometric Hydrogenation. In the absence of hydrogen, $H_4Ru_4(CO)_{12}$ reacted with ethylene at 72 °C to form ethane. The yields of ethane produced during the course of reaction are shown in Figure 2. The hydrogenation of ethylene took place without any induction periods and was complete within 60 min to give about two molecules of ethane per molecule of $H_4Ru_4(CO)_{12}$, which indicates that all hydride ligands on the ruthenium cluster transfer into ethylene molecules. The rate of stoichiometric hydrogenation was not affected by changing the pressure of ethylene in the range of 30–300 torr.

Catalytic Hydrogenation. The $H_4Ru_4(CO)_{12}$ acts as a powerful catalyst for the hydrogenation of ethylene in the

(14) Slater, S.; Muetterties, E. L. *Inorg. Chem.* **1980**, *19*, 3337.
(15) Ryan, R. C.; Pittman, C. U., Jr.; O'Connor, J. P. *J. Am. Chem. Soc.* **1977**, *99*, 1986.
(16) Pierantozzi, R.; Mcquade, K. J.; Gates, B. C., preprint B 18 of the 5th International Congress on Catalysis, Tokyo, 1980.
(17) Knox, S. A. R.; Koepke, J. W.; Andrews, M. A.; Kaesz, H. D. *J. Am. Chem. Soc.* **1975**, *97*, 3942.

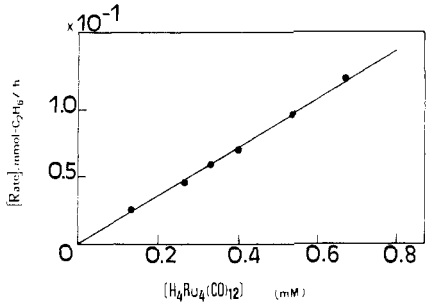

Figure 4. Rate of catalytic hydrogenation as a function of the $H_4Ru_4(CO)_{12}$ concentration (72 °C, $P_{C_2H_4}$ = 100 torr, P_{H_2} = 100 torr, and heptane solution (5 mL)).

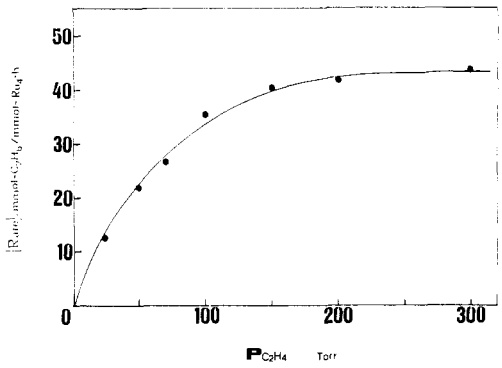

Figure 5. Rate of catalytic hydrogenation as a function of ethylene pressure (72 °C, P_{H_2} = 100 torr, and 0.4 mM solution of $H_4Ru_4(CO)_{12}$ (5 mL)).

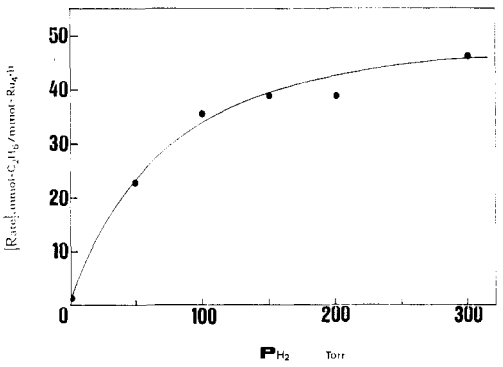

Figure 6. Rate of catalytic hydrogenation as a function of hydrogen pressure (72 °C, $P_{C_2H_4}$ = 100 torr, and 0.4 mM solution of $H_4Ru_4(CO)_{12}$ (5 mL)).

presence of excess hydrogen. Figure 3 shows a typical time course of the catalytic hydrogenation of ethylene at 72 °C. The ethane yield was proportional to the reaction time for at least 120 min. The rate of catalytic hydrogenation was determined from the slope of the linear curve. In all cases, the hydrogenation was performed in the range of low conversions of ethylene and hydrogen up to several percent.

The hydrogenation rate was first order with respect to the concentration of $H_4Ru_4(CO)_{12}$, as shown in Figure 4. Figure 5 shows the relation between the hydrogenation rate and the ethylene pressure. The hydrogenation rate increased to a constant value with increasing the ethylene pressure. Figure 6 shows the dependence of the hydrogen pressure on the hydrogenation rate. The rate at 0 torr of hydrogen pressure corresponds to the initial rate of the stoichiometric hydrogenation. It is worth noting that the presence of hydrogen accelerates the rate of hydrogenation.

The effect of carbon monoxide on the hydrogenation rate were examined at 72 °C. Various amounts of CO were added in the reactor during the course of catalytic hydrogenation of

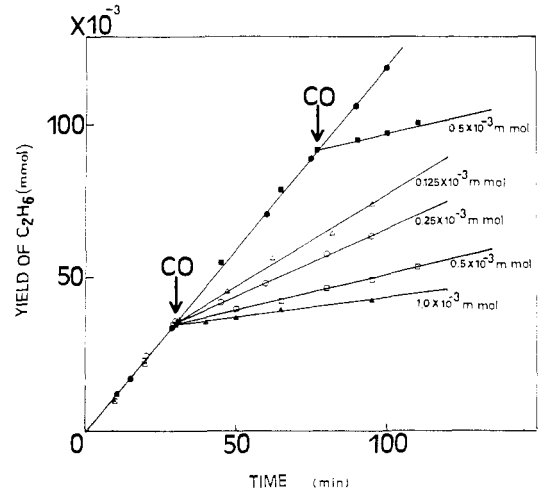

Figure 7. Changes in the yield of C_2H_6 induced by the addition of CO during the catalytic hydrogenation of ethylene (72 °C, $P_{C_2H_4}$ = 100 torr, P_{H_2} = 100 torr, and 0.4 mM solution of $H_4Ru_4(CO)_{12}$ (5 mL)). The amounts of CO added are shown in the figure.

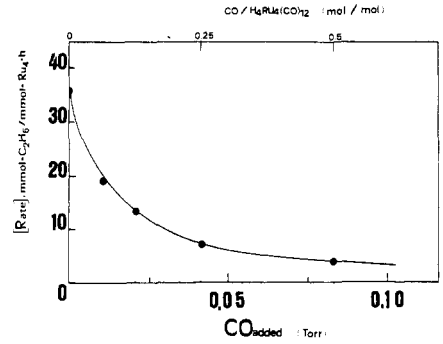

Figure 8. Relation between rate of catalytic hydrogenation and pressure of CO added.

ethylene. As shown in Figure 7, the addition of CO caused sudden suppression in the hydrogenation rate. Figure 8 shows the inverse relation between the hydrogenation rate and the pressure of CO added. At the end of reaction involving 1.0 × 10^{-3} mmol of CO in which the catalytic activity almost disappeared, the infrared and electron absorption spectra of catalyst solution were recorded at room temperature. The detectable Ru compound was $H_4Ru_4(CO)_{12}$, and the recovery of $H_4Ru_4(CO)_{12}$ was found to be almost 100% within experimental error.

So that the nature of the catalyst could be clarified, electron absorption spectra of catalyst solution were recorded at 72 ± 2 °C. A heptane solution of $H_4Ru_4(CO)_{12}$ exhibits an intense maximum at 366 nm (ϵ_m 17 800 M^{-1} cm^{-1}) in the near-UV region under an argon atmosphere. When hydrogen gas of 300 torr was exposed to the solution, the absorption maximum was red shifted toward 372 nm. The removal of hydrogen gas from the heptane solution caused a reversible change in the absorption maximum from 372 to 366 nm, indicative of a reversible reaction between $H_4Ru_4(CO)_{12}$ and H_2. Another attempt has been made to examine the absorption spectral changes during the stoichiometric hydrogenation of C_2H_4 with $H_4Ru_4(CO)_{12}$ in the absence of H_2. At the initial stage of the hydrogenation, the absorption maximum (365 nm) of the reaction solution under ethylene gas of 100 torr was almost identical with that of $H_4Ru_4(CO)_{12}$ solution under argon, although the band was broader. The production of ethane during the reaction resulted in gradual and irreversible spectral changes. When the stoichiometric hydrogenation was complete, the reaction solution exhibited a broad band at 360 nm

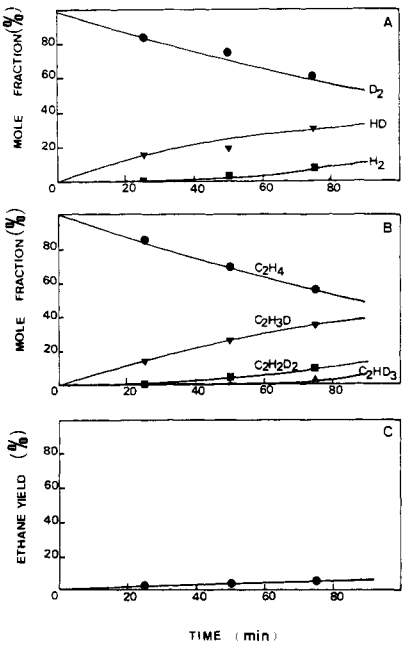

Figure 9. Deuterium distribution in reactants and conversion to ethane observed in the reaction of C_2H_4 with D_2 at 72 °C ($P_{C_2H_4}$ = 100 torr, P_{D_2} = 100 torr, and 0.4 mM solution of $D_4Ru_4(CO)_{12}$ (5 mL)).

and a shoulder at 430 nm. However, the ruthenium products arising from the reaction of $H_4Ru_4(CO)_{12}$ with C_2H_4 have not been identified.

Reaction Involving Deuterium. Deuterium-labeling experiments were carried out at 72 °C by using $D_4Ru_4(CO)_{12}$ in place of $H_4Ru_4(CO)_{12}$. (i) On exposing deuterium gas of 100 torr to heptane solution (0.4 mM) of $D_4Ru_4(CO)_{12}$, no hydrogen–deuterium exchange was observed in 240 min, indicating that solvent hydrogens do not participate in the hydrogenation process. However, in this experiment a small amount of CO was always detected from the mass spectra of gas components. (ii) When the mixture of deuterium gas of 50 torr and hydrogen gas of 50 torr was exposed for 60 min, gas composition of 33% H_2, 34% HD, and 33% D_2 was observed. The formation of HD clearly indicates that $D_4Ru_4(CO)_{12}$ catalyzes the H_2/D_2 exchange. (iii) The result in the reaction of ethylene with D_2 is shown in Figure 9. When D_2 was used in place of H_2, the rate of ethylene hydrogenation decreased and the kinetic isotope effect, i.e., k_H/k_D was 1.22 at 72 °C. A similar small isotope effect has been observed for the catalystic hydrogenation of decene-1 (k_H/k_D = 1.30) with μ_3-oxo-triruthenium acetate cluster complex.[6] Deuterium distribution was examined only in reactants since the conversion to ethane was too low. As shown in Figure 9, a hydrogen–deuterium exchange between reactants took place simultaneously with the hydrogenation of ethylene. Ethylene-d_1 (C_2H_3D) and HD were detected as main products in the initial stage of reaction. The rate of hydrogen–deuterium exchange between ethylene and D_2 was faster than the rate of ethane formation by at least 1 order of magnitude.

Discussion

Nature of Catalyst. The rate of catalytic hydrogenation of ethylene was proportional to the concentration of the catalyst precursor $H_4Ru_4(CO)_{12}$. Therefore, it is reasonable to assume that the tetranuclear cluster frameworks themselves provide the catalytic sites. Since the catalyst precursor $H_4Ru_4(CO)_{12}$ is coordinatively saturared, the first step in the catalytic cycle must involve a creation of vacant coordination sites without breaking up the cluster into mononuclear fragments. The formation of such vacant coordination sites may be achieved

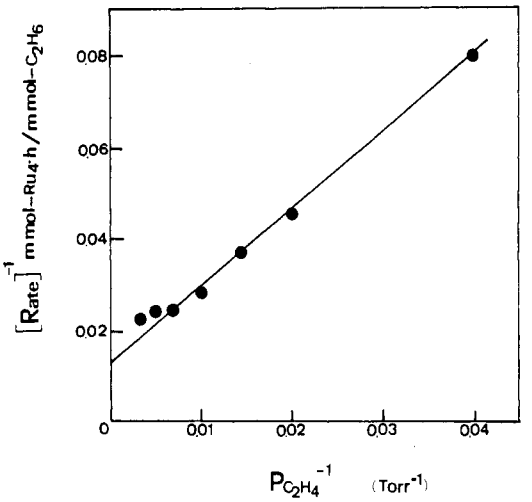

Figure 10. Plot of $[rate]^{-1}$ vs. $P_{C_2H_4}^{-1}$.

by the following two ways: (i) cleavage of one ruthenium–ruthenium bond resulting in an open butterfly structure

$$H_4Ru_4(CO)_{12} \rightleftharpoons H_4Ru_4(CO)_{12}^* \quad (1)$$

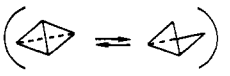

and (ii) dissociation of a ligand, specifically carbon monoxide

$$H_4Ru_4(CO)_{12} \overset{K_1}{\rightleftharpoons} H_4Ru_4(CO)_{11} + CO \quad (2)$$

Though we could not derive a definitive conclusion on the first step in the mechanism of this hydrogenation, the observed evolution of CO on exposing hydrogen to the heptane solution of $H_4Ru_4(CO)_{12}$ and the suppression of hydrogenation rate by excess CO appear to support a first step comprising CO dissociation ii. In addition, the mechanism involving CO dissociation ii is fully consistent with the kinetic data for the catalytic hydrogenation of ethylene, as discussed below.

Mechanism of Hydrogenation. The mechanism proposed for the catalytic hydrogenation of ethylene is outlined in eq 3–5. This mechanism is supported by the following experi-

$$H_4Ru(CO)_{11} + H_2 \overset{K_2}{\rightleftharpoons} H_6Ru_4(CO)_{11} \quad (3)$$

$$H_4Ru_4(CO)_{11} + C_2H_4 \overset{K_3}{\rightleftharpoons} H_3Ru_4(CO)_{11}(C_2H_5) \quad (4)$$

$$H_3Ru_4(CO)_{11}(C_2H_5) + H_2 \xrightarrow{k_4} H_4Ru_4(CO)_{11} + C_2H_6 \quad (5)$$

mental results. (i) The reversible spectral change (366 nm $\rightleftarrows$ 372 nm) of the heptane solution of $H_4Ru_4(CO)_{12}$ under argon and hydrogen appears to support the reversible reaction 3 giving $H_6Ru_4(CO)_{11}$ under H_2. In addition, a rapid H_2/D_2 exchange reaction to give HD in the presence of $D_4Ru_4(CO)_{12}$ can be rationalized in terms of hydride exchange on the ruthenium cluster framework through reaction 3. (ii) The reaction of ethylene with D_2 revealed that the exchange reaction of hydrogen–deuterium atoms between reactants takes place to give C_2H_3D and HD by a more rapid rate than that of ethane formation. It is reasonable to assume that an ethyltetraruthenium intermediate is present in the catalytic cycle and that the reverse reaction of eq 4 to give a free ethylene molecule is substantially faster than the formation of ethane via reaction 5. As described in the preceding section, the initial electron absorption spectrum of the $H_4Ru_4(CO)_{12}$ solution under C_2H_4 was almost identical with that of $H_4Ru_4(CO)_{12}$ solution under argon. The spectrum of the ethyltetraruthenium intermediate $H_3Ru_4(CO)_{11}(C_2H_5)$, which should be formed rapidly under C_2H_4, may be almost the same as that of

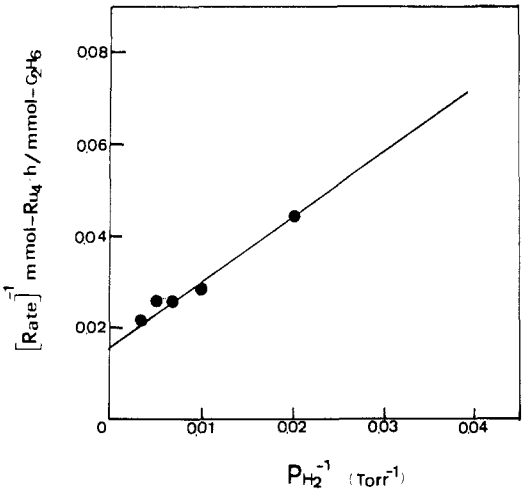

Figure 11. Plot of [rate]$^{-1}$ vs. $P_{H_2}^{-1}$.

$H_4Ru_4(CO)_{12}$. (iii) The observed acceleration of hydrogenation rate by the presence of hydrogen (see Figure 6) suggests that a hydrogenolysis reaction 5 is the predominant final step in the catalytic cycle of ethylene hydrogenation. In contrast, ethane must be formed through a slow transfer reaction of coordinated hydride to the ruthenium–ethyl bond in the stoichiometric reaction of $H_4Ru_4(CO)_{12}$ with ethylene, resulting in the decomposition of $H_4Ru_4(CO)_{12}$ in the absence of hydrogen. In the presence of excess hydrogen, the rate of the hydride transfer reaction is apparently negligible to that of hydrogenolysis reaction 5.

On the basis of the scheme outlined by steps 2–5, the rate of ethane formation in the presence of hydrogen is given by eq 6, where K_1, K_2, and K_3 are equilibrium constants of the

$$\frac{d[C_2H_6]}{dt} = \frac{k_4K_3[C_2H_4][H_2][Ru_4]_T}{1 + K_2[H_2] + K_3[C_2H_4] + [CO]/K_1} \quad (6)$$

respective steps 2–4, k_4 is rate constant for the hydrogenolysis step 5, $[Ru_4]_T$ denotes the total concentration of tetraruthenium cluster present, and $[H_2]$, $[C_2H_4]$, and [CO] refer to the free concentrations of these species. With the assumption that the concentrations of substrates in the catalyst

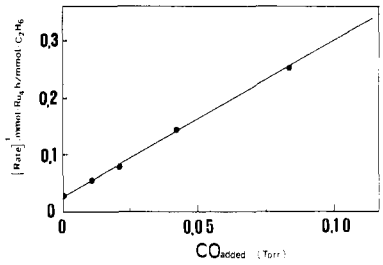

Figure 12. Plot of [rate]$^{-1}$ vs. P_{CO}.

solution are proportional to the respective partial pressures under the reaction conditions, eq 6 is rewritten as eq 7, where

$$\frac{d[C_2H_6]}{dt} = \frac{k_4'K_3'P_{C_2H_4}P_{H_2}[Ru_4]_T}{1 + K_2'P_{H_2} + K_3'P_{C_2H_4} + P_{CO}/K_1'} \quad (7)$$

new constants K_1', K_2', K_3', and k_4' involve the solubility constants of substrates in the catalyst solution. Equation 7 predicts that the rate is proportional to the total concentration of tetraruthenium cluster. This relation is confirmed by the result of Figure 4. Equation 7 when written in inverse form is given by eq 8. Equation 8 predicts that the respective plots

$$[Ru_4]_T\left(\frac{d[C_2H_6]}{dt}\right)^{-1} = \frac{1}{k_4'K_3'P_{H_2}P_{C_2H_4}} + \frac{K_2'}{k_4'K_3'P_{C_2H_4}} + \frac{1}{k_4'P_{H_2}} + \frac{P_{CO}}{k_4'K_1'K_3'P_{H_2}P_{C_2H_4}} \quad (8)$$

of $[Ru_4]_T(d[C_2H_6]/dt)^{-1}$ vs. $P_{C_2H_4}^{-1}$, $[Ru_4]_T(d[C_2H_6]/dt)^{-1}$ vs. $P_{H_2}^{-1}$, and $[Ru_4]_T(d[C_2H_6]/dt)^{-1}$ vs. P_{CO} should be linear. As Figures 10–12 show, kinetics results obtained in the catalytic hydrogenation of ethylene are in complete agreement with the above expression 8. From the values of the intercepts and the slopes of Figures 10–12, the values of K_1', K_2', K_3' and k_4' at 72 °C are estimated as $(5.4 \pm 1.6) \times 10^{-4}$ torr, $(1.0 \pm 0.3) \times 10^{-1}$ torr^{-1}, $(8.7 \pm 2.6) \times 10^{-2}$ torr^{-1}, and $(7.6 \pm 0.7) \times 10^{-1}$ h^{-1} torr^{-1}, respectively. Thus, our kinetic data support the scheme outlined by steps 2–5.

Acknowledgment. The authors wish to thank Professor Y. Ono for valuable discussions.

Registry No. $H_4Ru_4(CO)_{12}$, 34438-91-0; ethylene, 74-85-1.